Linear Analysis Tools for Edge and Scrape-off-Layer Plasmas

J. R. Myra

Lodestar Research Corp., 2400 Central Ave. P-5, Boulder, Colorado 80301

M. V. Umansky,

Lawrence Livermore National Laboratory, Livermore, CA 94550

June 2008

LODESTAR RESEARCH CORPORATION

2400 Central Avenue
Boulder, Colorado 80301

Linear Analysis Tools for Edge and Scrape-off-Layer Plasmas

J. R. Myra[1] and M. V. Umansky [2]

[1] Lodestar Research Corporation, Boulder, CO, USA

[2] Lawrence Livermore National Laboratory, Livermore, CA, USA

1. Introduction

The edge and scrape-off-layer region of a tokamak plasma is subject to well-known ideal and resistive instabilities that are driven by various curvature- and sheath- related mechanisms. While the boundary plasma is typically strongly turbulent in experiments, it is useful to have computational tools that can analyze the linear eigenmode structure, predict quantitative trends in growth rates and elucidate the underlying drive mechanisms. Furthermore, measurement of the linear growth rate of unstable modes emerging from a known, established equilibrium configuration can provide rigorous quantitative benchmarking of plasma turbulence codes. Because the tokamak edge physics community is becoming increasingly reliant on large-scale-simulation, rigorous verification and validation (V&V) of edge codes is critical. In this paper, we describe a suite of codes that can describe linearized, nonlocal (e.g. separatrix-spanning) modes in axisymmetric (realistic divertor), toroidal geometry. Results of benchmark comparisons are given for these codes, with each other and with analytical results. The inclusion of kinetic physics effects in 2DX is also discussed.

2. The BOUT and 2DX Codes

The BOUT code is a 3D fluid turbulence code that simulates plasma evolution in the boundary plasma.[1,2] BOUT handles complex magnetic topologies and implements full toroidal divertor geometry, including single and/or double null X-points. It is a "global" code (radially varying geometry, plasma profiles and mode structure). The fluid equations describing the plasma are evolved by an implicit time advancement scheme. BOUT is at a mature stage in its development, and details have been described elsewhere. For the linear mode studies described here, BOUT is run with the nonlinear terms turned off.

2DX is a new linear eigenvalue code for the boundary plasma that is under development. It extends the 1D (along B) eikonal codes BAL[3] (shooting) and MBAL[4] (matrix eigenvalue) to 2D. Axisymmetry allows a given toroidal mode to be studied in isolation. The 2DX algorithm is to project the unknown eigenfunctions onto a 2D (radial, poloidal) grid

using basis modes (e.g. Fourier) or spatial discretization and cast the equations and boundary conditions as operators in this space. Standard eigen-system solvers then yield the eigenvalues (linear growth rates γ) and eigenfunctions (ξ)

$$M\xi = \gamma\xi \qquad (1)$$

where M contains blocks for the interactions of each of the field variables (e.g. n and Φ for the model described in Sec. 3)

The 2DX code is modular and achieves good separation of physics equations, coordinates, basis sets, and numerical methods. 2DX first defines elementary 1D operators for the given basis representation. Physics operators such as $\nabla_\perp$, $\nabla_\parallel$, are then formed for each coordinate system – both field-line-following (FLF) and geometrical angle (GA). Finally, the physics model is employed to construct the matrix elements.

3. Verification Models and Test Results

Five verification tests were designed to extend earlier verification studies for BOUT[5], to provide verification of 2DX, and to take a step towards the creation of accepted verification standards for edge turbulence codes in general. Four of these tests were done in the 2-field (potential Φ, density n) resistive ballooning model given (in normalized form) by

$$\frac{\partial}{\partial t}\nabla_\perp^2\Phi = -\frac{\sigma}{n_0}\nabla_\parallel^2\Phi + \frac{2}{n_0}\mathbf{b}\times\kappa\cdot\nabla n \qquad (2)$$

$$\frac{\partial n}{\partial t} = -\mathbf{b}\times\nabla\Phi\cdot\mathbf{e}_x\frac{\partial n_0}{\partial x} \qquad (3)$$

where $n_0(x)$ is a specified equilibrium density profile and x is a radial variable. Here σ is the Spitzer conductivity and κ is the curvature. The boundary conditions for the model are periodic in geometrical poloidal angle θ in the closed flux surface region, and sheath boundary conditions in the SOL, i.e. at the sheath entrance

$$J_\parallel \equiv -\sigma_\parallel\nabla_\parallel\Phi = \pm\frac{n_0 e^2 c_s}{T_0}\Phi \qquad (4)$$

Test 1, *Resistive interchange in the edge*, verified the curvature drive term, radial derivative and radial mode structure in slab geometry. Test 2, *Shearless resistive ballooning in the edge*, tested the mode structure in θ and the parallel derivatives in $\sigma\nabla_\parallel^2\Phi$. It also tested the implementation of phase-shift-periodic boundary conditions for the FLF coordinate system (i.e. "twist-shift" boundary conditions compatible with the ballooning representation). Test 3, *Sheared resistive ballooning in the edge*, tested the coupling of the radial (x) and parallel (y or θ) mode structure in a more complicated magnetic geometry. For test 4, *Nedospasov mode in the SOL*, we considered a plasma slab with sheath boundary conditions. Three cases were run

to allow the boundary condition to transition from a conducting to an insulating sheath. Finally, Test 5, *Conducting wall mode in the SOL*, employed a slight extension of Eqs. (2) – (4), and allowed a more comprehensive test of sheath boundary conditions and their coupling to radially varying profiles. This model relies on a completely different instability mechanism, unrelated to magnetic field line curvature.[6] More details of the tests and results are given in a technical report.[7] Fig. 1 shows a sample result for Test 2.
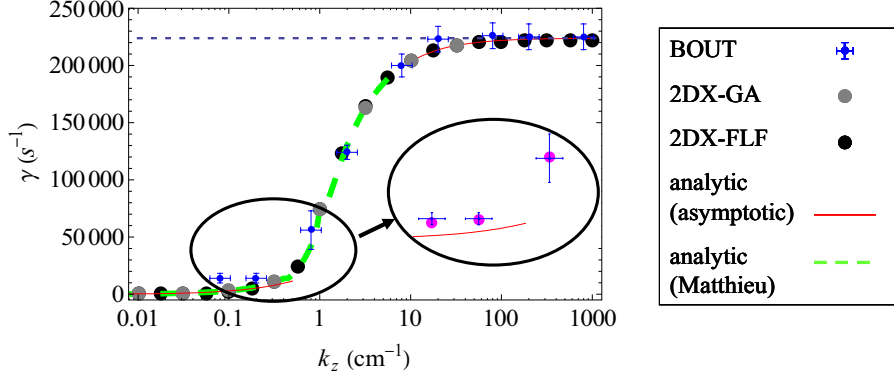

Fig. 1 Growth rate γ vs. binormal wavevector k_z for the resistive ballooning instability in a shearless annulus. 2DX code results using both GA coordinates and FLF coordinates are shown. The crosses are measured growth rates from BOUT with estimated error bars. The green dashed curve is the numerical solution of a Mathieu function dispersion relation which solves the model, the red dashed curves are the small and large k_z analytical solutions, and the dotted horizontal line is the local resistive ballooning limit. Initial 2DX runs used an analytical equilibrium. Agreement with BOUT is improved at low k_z (inset) when 2DX (magenta) and BOUT use the same numerical equilibrium.

4. Divertor Geometry and Kinetic Physics in 2DX

The capability to describe full divertor geometry in 2DX has been achieved by importing magnetic geometry and plasma profile data from HDF files that are created from the same input used by the BOUT pre-processor. 2DX carries out independent pre-processor calculations (e.g. of curvatures) providing an additional verification check. Fig. 2 shows sample 2DX results for different toroidal mode numbers in realistic DIII-D geometry.

A proof-of-principle demonstration of kinetic physics extensions in 2DX has also been carried out. We replaced the Braginskii constant σ in Eq. (2) with the corresponding Z-function closure for $J_\parallel$ from kinetic theory for the electrons, with $\zeta = (\omega+i\nu)/k_\parallel v_e$,

$$\sigma_\parallel = \frac{\omega}{4\pi i}\frac{1}{k_\parallel^2\lambda_{de}^2}\left(1+\zeta Z(\zeta)\right) \tag{5}$$

Since the matrix M now depends on the eigenvalue γ through the Z-function argument ζ, Eq. (1) was iterated to convergence using eigenvalue perturbation theory together with a
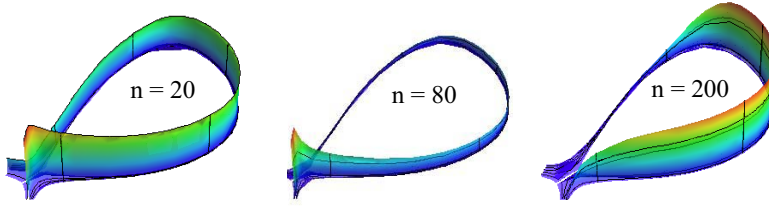
Fig. 2 Sample 2DX eigenfunctions for a DIII-D case, illustrating different toroidal mode numbers, n, and different interactions with the X-points and the sheaths

Newton-type iteration. The iteration rule to get from a given guess γ_0 to the next refinement γ_1 is given by

$$\gamma_1 = \gamma_0 - \frac{F[M(\gamma_0)] - \gamma_0}{\left\langle \xi_0 \left| \frac{\partial M}{\partial \gamma} \xi_0 \right\rangle - 1\right.} \qquad (6)$$
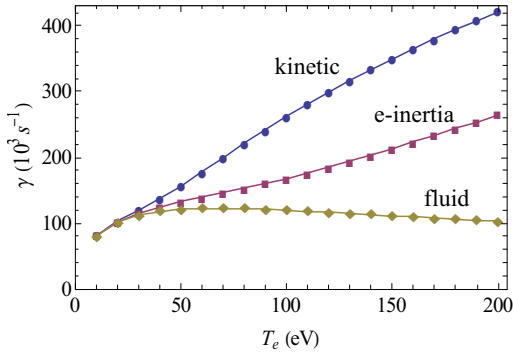

Fig. 3 Demonstration of kinetic physics in 2DX. Shown are growth rate $\gamma(10^3/s)$ vs. T_e(eV) for the three cases: kinetic (top blue curve), fluid with electron inertia (middle plum curve) and collisional fluid (lower olive curve). Note that for small T_e all the models are equivalent, but at large T_e kinetic physics adds additional instability drive.

5. Discussion

Although the present tests provide a significant level of verification, additional tests that include more general physics models in divertor geometry are highly desirable. This will require extensions to 2DX. In addition to benchmarking, there are many possible stand-alone applications for 2DX such as quasilinear flux comparisons, plasma shaping and geometry studies, and ELM and quasi-coherent edge mode stability.

[1] X.Q. Xu and R.H. Cohen, Contrib. Plasma Phys. **36**, 158 (1998).
[2] M.V. Umansky et al., Contrib. Plasma Phys. **44**, 182 (2004).
[3] J. R. Myra, D.A. D'Ippolito, X.Q. Xu and R.H. Cohen, Phys. Plasmas **7**, 4622 (2000).
[4] J. R. Myra, D.A. D'Ippolito and X.Q. Xu, Phys. Plasmas **9**, 1637 (2002).
[5] M. V. Umansky, R. H. Cohen, L. L. LoDestro, and X. Q. Xu, Contrib. Plasma Phys. **48**, 27 (2008).
[6] H. L. Berk, R. H. Cohen, D. D. Ryutov, Yu. A. Tsidulko, and X. Q. Xu, Nucl. Fusion **33**, 263 (1993).
[7] J. R. Myra and M. Umansky, Lodestar Report #LRC-08-120, April, 2008,
      http://www.lodestar.com/LRCreports/Linear%20Analysis%20LRC%20Report.pdf